

## Holography with Low-Energy Electrons

Hans-Werner Fink, Werner Stocker, and Heinz Schmid

Zurich Research Laboratory, IBM Research Division, 8803 Rüschlikon, Switzerland

(Received 30 May 1990)

We have employed an ultrasharp tip, prepared by field-ion techniques, as a coherent point source of low-energy electrons. The source, which constitutes the origin of a spherical electron wave, is positioned close to small carbon fibers, at which some of the electrons are elastically scattered. At macroscopic distances a hologram is observed, which arises from the interference of the scattered electrons with the reference wave. The high magnification of the interference pattern is brought about purely by geometric projection. No electron lenses are employed and, thus, the high-resolution microscopic information gained by this novel technique is not affected by aberrations.

PACS numbers: 42.40.-i, 07.80.+x, 34.80.-i, 41.80.-y

The concept of holography was introduced by Gabor in 1948.<sup>1</sup> His aim was to improve the resolution of electron microscopes by recording the amplitude distribution contained in an interference pattern brought about by interaction of a wave scattered by an object and a coherent reference wave. In principle, the information contained in this pattern fully represents the object, because the phase information is not lost, as in conventional electron microscopy. Gabor also envisioned that this pioneering concept would circumvent those limitations of electron microscopes arising from the inherent aberrations of their lens systems. The invention of the laser, which produces a coherent and bright light source, then converted this ingenious concept into a practical tool, that has since been used in a wide field of applications.<sup>2</sup>

The development of electron holography has been slow due to the lack of sources with sufficient brightness and coherence. Moreover, the relatively poor performance of electron lenses compared to that of optical lenses imposed additional problems. Only recently has the work done by the Tübingen group<sup>3</sup> demonstrated high-resolution electron holography and, with this, established a place for holography within the community of high-energy electron microscopy techniques.

However, some of the problems intrinsic in focused high-energy electron beams are still inherent to this approach: These include lens aberrations, brightness limitations, and a weak phase shift on scattering of high-energy electrons at carbon atoms, the vital building block in organic materials.

We would like to present here a novel experimental scheme for electron holography. It draws on the coherence and brightness properties of waves from point sources of both electrons and noble-gas ions: Such waves arise from sources that can ultimately be shaped into an atomic pyramid terminated by just one individual atom.<sup>4</sup> The atomic-sized emission volume of these sources and the correspondingly low extraction voltages enable us to produce a coherent low-energy electron beam for use in a lens-free setup for in-line holography.

The experimental design of our lens-free projection microscope is illustrated in Fig. 1. By employing fine mechanical manipulation adopted from scanning tunneling microscopy technology,<sup>5</sup> an ultrasharp tip emitter is brought into close proximity to a partly transparent carbon film, at ground potential with respect to the emitter. Down to submicron separations  $d$ , between the tip and sample, the carbon film constitutes an equipotential surface which ensures that a rotationally symmetric emission cone originates from the point source. At a channel-plate detector, placed at a macroscopic distance  $D$  behind the sample, a magnified projection image of the foil and structures within the holes can be observed, with high image contrast and within a short time.<sup>6</sup> The magnification is simply given by geometry, and is proportional to  $D/d$ . Since most of the electrons emitted from the source are used to form the image, total emission currents between 20 and 100 pA are sufficient to obtain high-contrast image information.

A sequence showing the approach of the emitting source to the object under investigation is shown in Fig. 2. The subsequent decrease of the distance between emitter tip and sample leads to an increased magnification of up to 150000 times, in the sequence shown

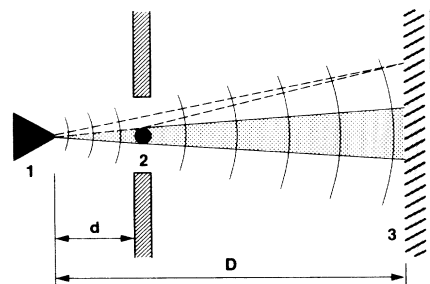


FIG. 1. Schematic representation of the projection microscope: 1, source for electrons; 2, planar perforated foil with sample objects crossing the holes; and 3, two-dimensional electron detector.

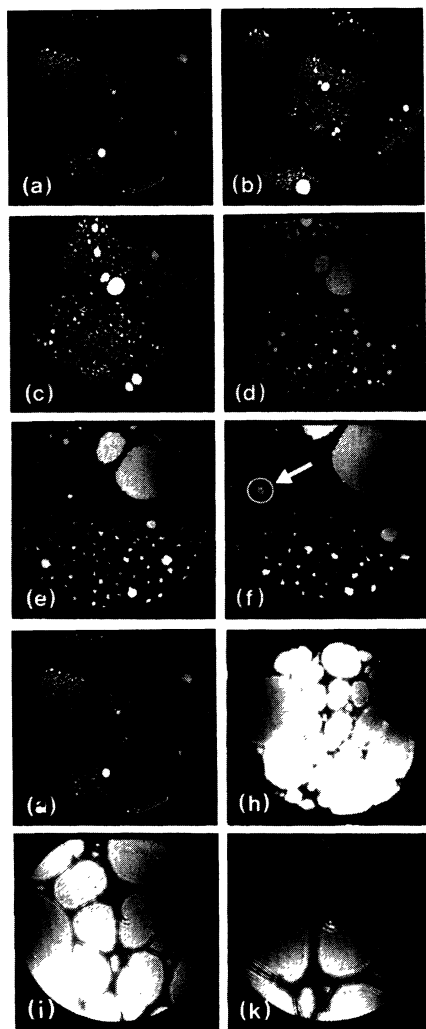


FIG. 2. Sequence showing an approach between the source and the perforated foil. The sequence starts (a) with a distance between the source and sample of  $482 \mu\text{m}$ . An extraction voltage of  $189 \text{ V}$  between the tip and sample is needed to draw a  $0.5\text{-nA}$  current, which forms the projection image at the channel-plate screen assembly,  $11 \text{ cm}$  away. The carbon foil is supported by a  $40\text{-}\mu\text{m}$  grid, apparent in (a) and (b) at low magnification. During the approach, the source-sample distance decreases, as well as the emission voltage, leading to more highly magnified images. In the following, the electron energies as well as the diameter of the field of view are quoted: (a)  $189 \text{ eV}$ ,  $175 \mu\text{m}$ ; (b)  $176 \text{ eV}$ ,  $131 \mu\text{m}$ ; (c)  $160 \text{ eV}$ ,  $78 \mu\text{m}$ ; (d)  $139 \text{ eV}$ ,  $37 \mu\text{m}$ ; (e)  $122 \text{ eV}$ ,  $16 \mu\text{m}$ ; (f)  $114 \text{ eV}$ ,  $11 \mu\text{m}$ ; (g)  $90 \text{ eV}$ ,  $2.4 \mu\text{m}$ ; (h)  $80 \text{ eV}$ ,  $1.0 \mu\text{m}$ ; (i)  $71 \text{ eV}$ ,  $0.5 \mu\text{m}$ ; (k)  $65 \text{ eV}$ ,  $0.27 \mu\text{m}$ .

here. With increasing magnification, the emission voltage applied to the tip decreases, due to the shorter source-sample distance. An electric field at the tip leading to an electron current of  $0.5 \text{ nA}$  is obtained at  $65\text{-V}$  potential difference between tip and sample at submicron distances, while at a macroscopic distance of  $0.5 \text{ mm}$ ,  $190 \text{ V}$  are required to draw the same emission current

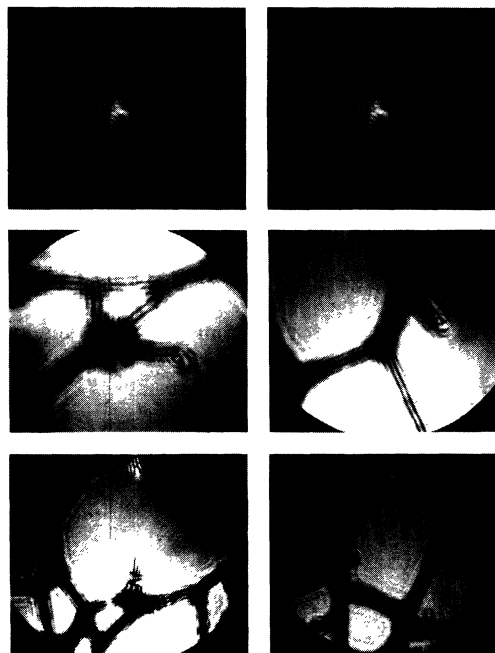


FIG. 3. A set of holograms taken with differently shaped carbon fibers; typical fiber diameters are between  $10$  and  $20 \text{ nm}$ .

from the tip.

In this way, images of carbon fibers exhibiting widths of about  $10\text{--}20 \text{ nm}$  are imaged, as apparent in Fig. 2. As long as the magnification has not reached a certain value, we obtain a shadow image, with contrast given by absorption of electrons at the fibers. At magnifications exceeding  $50000$ , the projection images turn into holograms with interference contrast, provided a sufficiently coherent initial electron beam is employed.

The projection microscope<sup>6</sup> becomes an interference microscope when the initial beam of low-energy electrons is coherent. Another prerequisite, as well as providing a coherent beam, is the need to observe the interference pattern on a finite resolution detector. To achieve this, the magnification has to be improved by reducing the distance between source and sample.

At present, we find that the observability of interference effects is not limited by the size of the emitter, which we can ultimately shape to a single-atom tip.<sup>4</sup> Limitations arise from the poor coherence of the initial electron beam, due to the relative position between emitter and sample remaining insufficiently constant, which, for all practical purposes, is equivalent to a more extensive source. Moreover, external ac magnetic fields influence the trajectories of the low-energy electrons. Improvements in vibration insulation and shielding of external magnetic fields, however, have provided sufficient coherence to observe interference effects with electrons of low energies.

With our test sample of small carbon fibers, in-line



FIG. 4. Interference fringes from a linear carbon fiber taken at two different electron energies (wavelengths) of 21 eV (left-hand side) and 26 eV (right-hand side).

holograms from electrons with energies between 21 and 80 eV have been observed, as shown in Fig. 3. Searching for the smallest objects in our sample is not a time-consuming effort, owing to the "real time" imaging capability and the wide scan range of the instrument. The smallest objects found were fibers exhibiting widths of the order of 10–20 nm. A set of holograms taken with differently shaped and arranged fibers is shown in Fig. 3.

The patterns of Fig. 3 can be interpreted by following Gabor's original concept of holography.<sup>1</sup> The ultrasharp tip is regarded as the origin of a spherical wave evolving towards the sample. Part of the wave passes the sample at a sufficiently large distance, such that no (or negligible) interaction with the object occurs, or it is transmitted by the object without being scattered. This fraction constitutes the reference wave. The other part of the low-energy electron wave interacts with the object and is elastically scattered. The two wave fields interfere with each other behind the object, due to phase shifts between the reference and object wave, caused by scattering. Both waves originated from the same point source, which ensures the coherence. At a far-away detector, this interference pattern can be observed with high magnification. Two holograms of the same fiber, taken at 21- and 26-eV electron energies, are shown in Fig. 4: They have been imaged with the same magnification. As expected from the different de Broglie wavelengths, the maxima in the patterns are separated by 0.80 nm (21 eV) and 0.72 nm (26 eV), corresponding to wavelengths of 0.266 and

0.239 nm, respectively.

We have shown that in-line holography with low-energy electrons is possible, at present with energies as low as 21 eV. Since the low energy of the electrons can be associated with a scattering mechanism entirely different from those in other microscopies, information not available from older microscopy tools is anticipated. Another unique feature is the high rate of gathering pictures, since almost all electrons emitted from the source contribute to the pattern. This will be of significant benefit in observing dynamic processes with high time resolution.

The reconstruction of the holograms, or, more precisely, the evaluation of the wave front at the object has not been addressed in this Letter. The principle, however, is straightforward: The hologram will have to be illuminated by a spherical wave analogous to the radiation used in the actual experiment. This will have to be done using numerical methods. Recent calculations by Lang, Yacoby, and Imry<sup>7</sup> on field emission from single adsorbed atoms suggest subatomic virtual source sizes, and provide information on trajectories that should be helpful in modeling the source for the reconstruction task. Although there is still a great deal to be done and to be understood, we view the prospects of this new tool as promising.

We are grateful to Dr. Roger Morin, CNRS-CRMC2 Marseille, Professor Hannes Lichte, University of Tübingen, and Professor Elmar Zeitler, Fritz-Haber Institut der Max-Planck Gesellschaft, Berlin, for fruitful discussions.

<sup>1</sup>D. Gabor, *Nature (London)* **161**, 777 (1948).

<sup>2</sup>G. W. Stroke, *An Introduction to Coherent Optics and Holography* (Academic, New York, 1969).

<sup>3</sup>For an overview, see H. Lichte, *Ultramicroscopy* **20**, 293 (1986), and references therein.

<sup>4</sup>H.-W. Fink, *Phys. Scr.* **38**, 260 (1988).

<sup>5</sup>G. Binnig and H. Rohrer, *Helv. Phys. Acta* **55**, 726 (1982).

<sup>6</sup>W. Stocker, H.-W. Fink, and R. Morin, *Ultramicroscopy* **31**, 379 (1989).

<sup>7</sup>N. D. Lang, A. Yacoby, and Y. Imry, *Phys. Rev. Lett.* **63**, 1499 (1989).

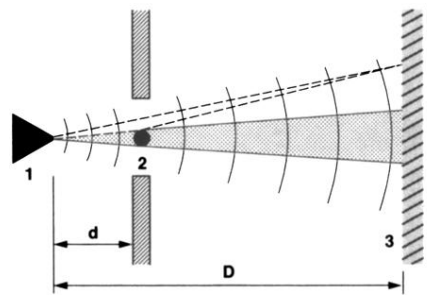


FIG. 1. Schematic representation of the projection microscope: 1, source for electrons; 2, planar perforated foil with sample objects crossing the holes; and 3, two-dimensional electron detector.

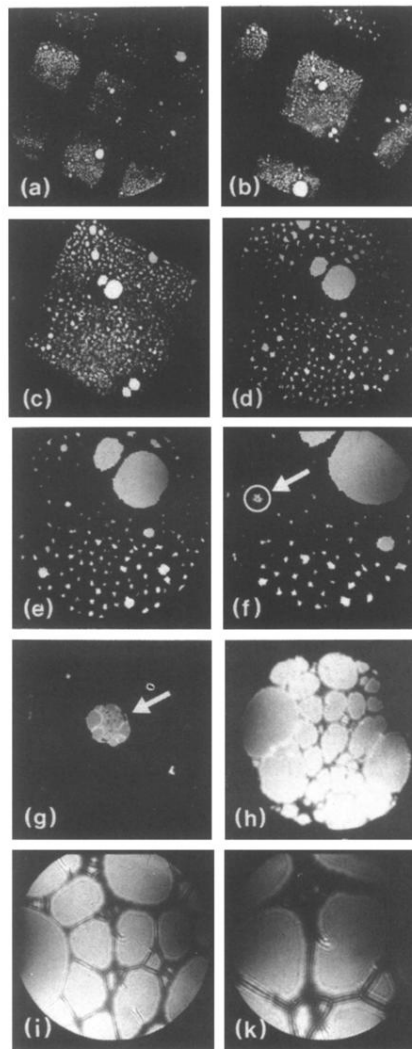


FIG. 2. Sequence showing an approach between the source and the perforated foil. The sequence starts (a) with a distance between the source and sample of  $482\ \mu\text{m}$ . An extraction voltage of  $189\ \text{V}$  between the tip and sample is needed to draw a  $0.5\text{-nA}$  current, which forms the projection image at the channel-plate screen assembly,  $11\ \text{cm}$  away. The carbon foil is supported by a  $40\text{-}\mu\text{m}$  grid, apparent in (a) and (b) at low magnification. During the approach, the source-sample distance decreases, as well as the emission voltage, leading to more highly magnified images. In the following, the electron energies as well as the diameter of the field of view are quoted: (a)  $189\ \text{eV}$ ,  $175\ \mu\text{m}$ ; (b)  $176\ \text{eV}$ ,  $131\ \mu\text{m}$ ; (c)  $160\ \text{eV}$ ,  $78\ \mu\text{m}$ ; (d)  $139\ \text{eV}$ ,  $37\ \mu\text{m}$ ; (e)  $122\ \text{eV}$ ,  $16\ \mu\text{m}$ ; (f)  $114\ \text{eV}$ ,  $11\ \mu\text{m}$ ; (g)  $90\ \text{eV}$ ,  $2.4\ \mu\text{m}$ ; (h)  $80\ \text{eV}$ ,  $1.0\ \mu\text{m}$ ; (i)  $71\ \text{eV}$ ,  $0.5\ \mu\text{m}$ ; (k)  $65\ \text{eV}$ ,  $0.27\ \mu\text{m}$ .

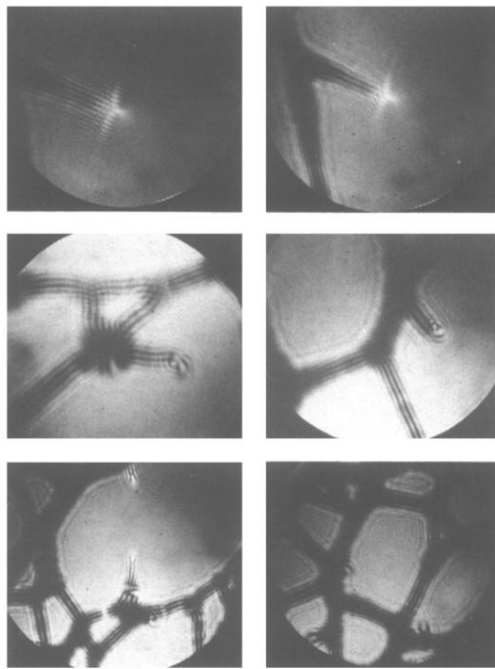


FIG. 3. A set of holograms taken with differently shaped carbon fibers; typical fiber diameters are between 10 and 20 nm.

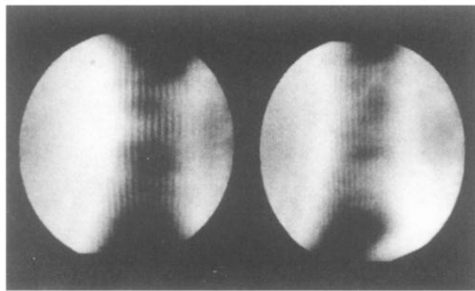


FIG. 4. Interference fringes from a linear carbon fiber taken at two different electron energies (wavelengths) of 21 eV (left-hand side) and 26 eV (right-hand side).